



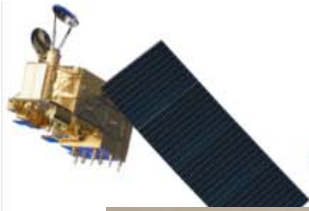
Progress on FY-3/MWRI FCDR

Shengli Wu, Qifeng Lu, Fenglin Sun, Wei Zhang
National Satellite Meteorological Center

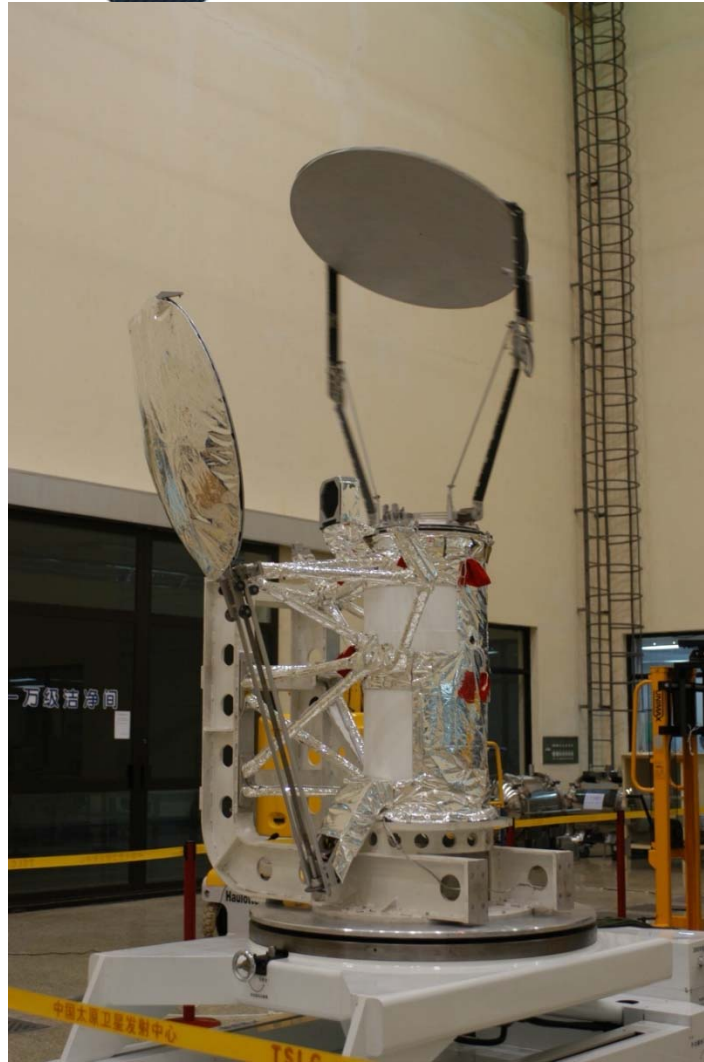
Hongxin Xu, Jiakai He
Shanghai Institute of Space Communication Technology

GSICS MWSG
2021.01.21





FY-3/MWRI Introduction



Frequency(GHz)	10.65	18.7	23.8	36.5	89
Polarization	V.H	V.H	V.H	V.H	V.H
Band Width(MHz)	180	200	400	900	2×2300
NeDT(k)	0.5	0.5	0.5	0.5	0.8
Accuracy(k)	2.0	2.0	2.0	2.0	2.0
BT Range(k)	3~340				
Scan Points	266(1.8s)				
Black Body Stability	0.3K				
Nonlinear	<1K				
Main Beam	≥90%				
Resolution ≤(km×km)	51×85	30×50	27×45	18×30	9×15
Beam of different Channel	<0.07°				
Scan	Conic				
Orbit Width(Km)	≥1400				
Antenna angle(°)	45				
Scan Period(s)	1.8±0.1 (1.7/2.0)				
Scan Period Stability(ms)	≤0.36ms* (2 Scan lines)				
	≤1ms(30 minutes)				





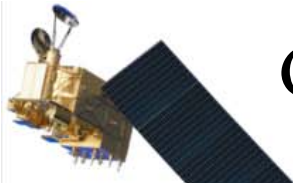
Current Status and Future Plan

在轨运行微波成像仪	2010年			2011年			2012年			2013年			2014年			2015年			2016年			2017年			2018年			2019年			2020年		
	Q1	Q2	Q3	Q1	Q2	Q3	Q1	Q2	Q3	Q1	Q2	Q3	Q1	Q2	Q3	Q1	Q2	Q3	Q1	Q2	Q3	Q1	Q2	Q3	Q1	Q2	Q3	Q1	Q2	Q3	Q1	Q2	Q3
FY-3B/MWRI	[Yellow bar]																																
FY-3C/MWRI	[Grey bar]																																
FY-3D/MWRI	[Green bar]																																

2021:FY-3F(Morning orbit, Antenna size: 1.8m);
2022:FY-3P(Low orbit, Antenna size: 1.6m);
2023:FY-3G(Afternoon orbit, Antenna size: 1.8m);
Antenna performance and NedT improved based on FY-3 02

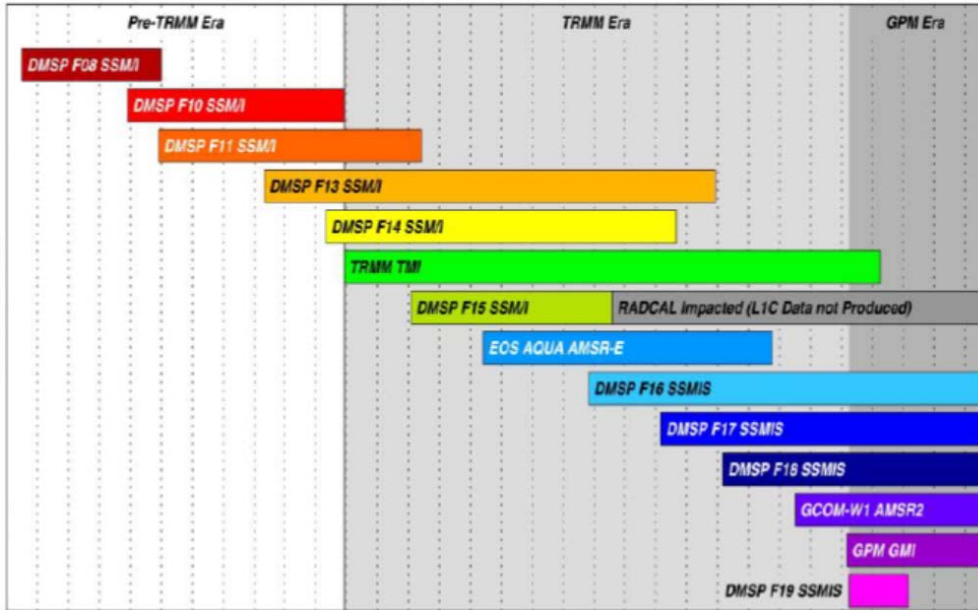


	FY-3A/B/C/D MWRI	FY-3F/G/P MWRI
Frequency (GHz)	10/18/23/36/89	10/18/23/36/50/89/ 18/166/183
Antenna (m)	1	1.8/1.6
NedT (K)	0.8/1.0	0.5/0.8
Accuracy (K)	2.0	0.8/1.2
Co-location (Km)	/	2
Main beam	0.9	0.95

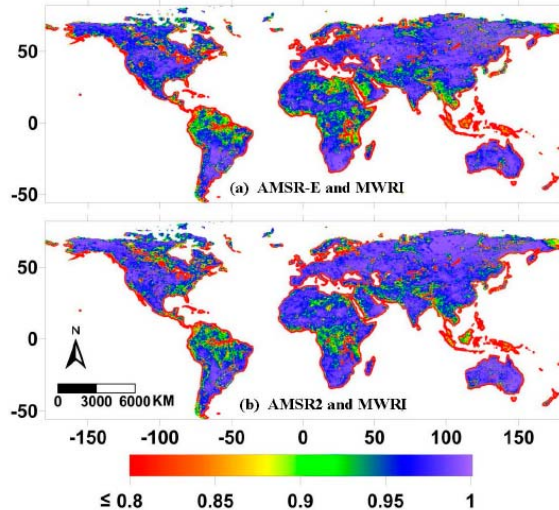
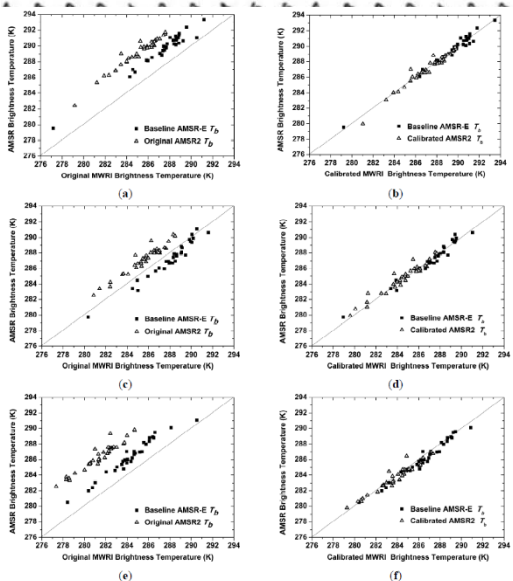
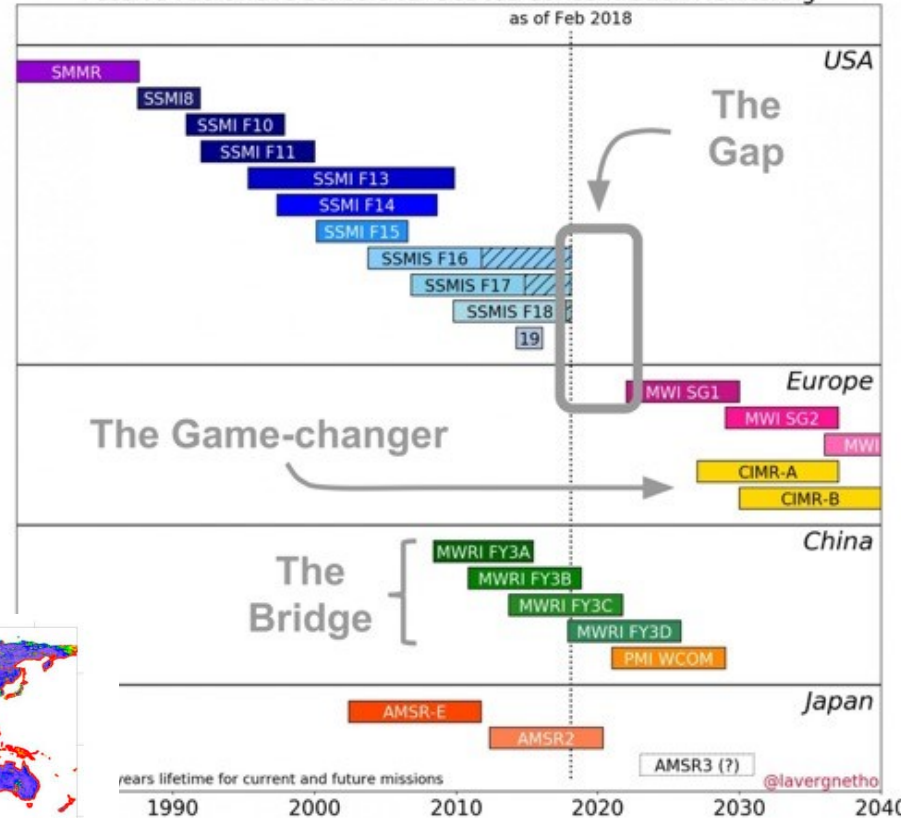


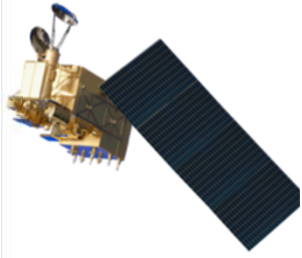
Global Radiometer(Imager) History and Future

Level 1C Dataset of Conical-Scanning Window Channel Radiometers



Passive Microwave sensors for Sea Ice Concentration Monitoring





GMI

Channel	At launch η	V04 η	ΔT_b at 200 K
10.65 V-pol	0.94435	0.95404	1.94
10.65 H-pol	0.94369	0.95404	2.07
18.7 V-pol	0.93968	0.95603	3.27
18.7 H-pol	0.94082	0.95603	3.04
23.8 V-pol	0.96601	0.97075	0.95
36.64 V-pol	0.9959	0.99535	-0.11
36.64 H-pol	0.9959	0.99535	-0.11
89.0 V-pol	0.9981	0.99734	-0.15
89.0 H-pol	0.9981	0.99734	-0.15
166.0 V-pol	1.0	0.98814	-2.37
166.0 H-pol	1.0	0.98814	-2.37
183.31 \pm 3 V-pol	1.0	0.99212	-1.58
183.31 \pm 7 V-pol	1.0	0.99212	-1.58

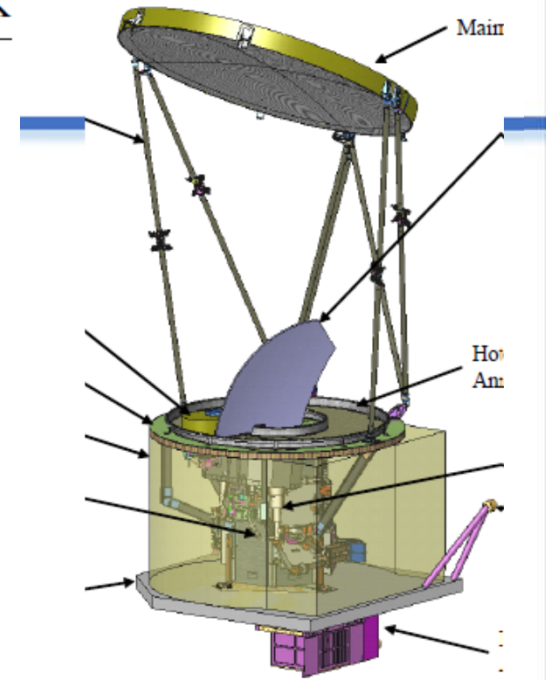


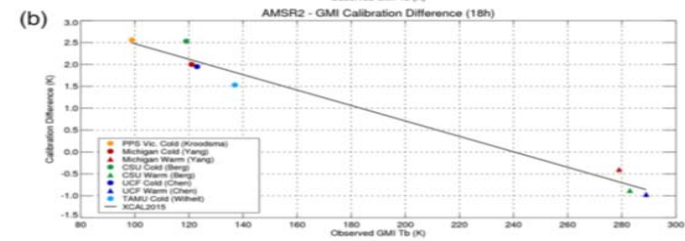
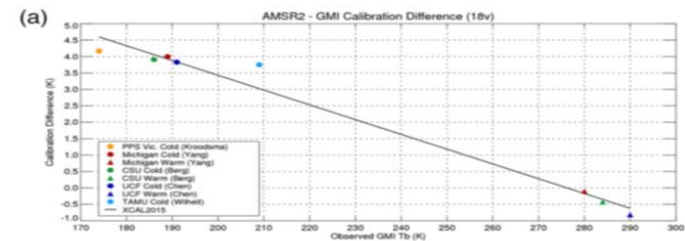
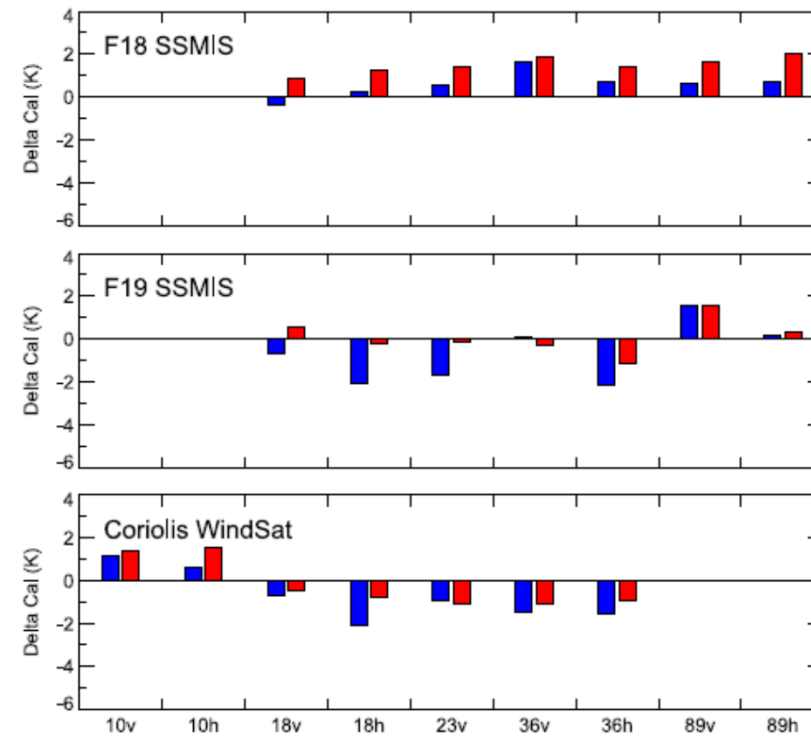
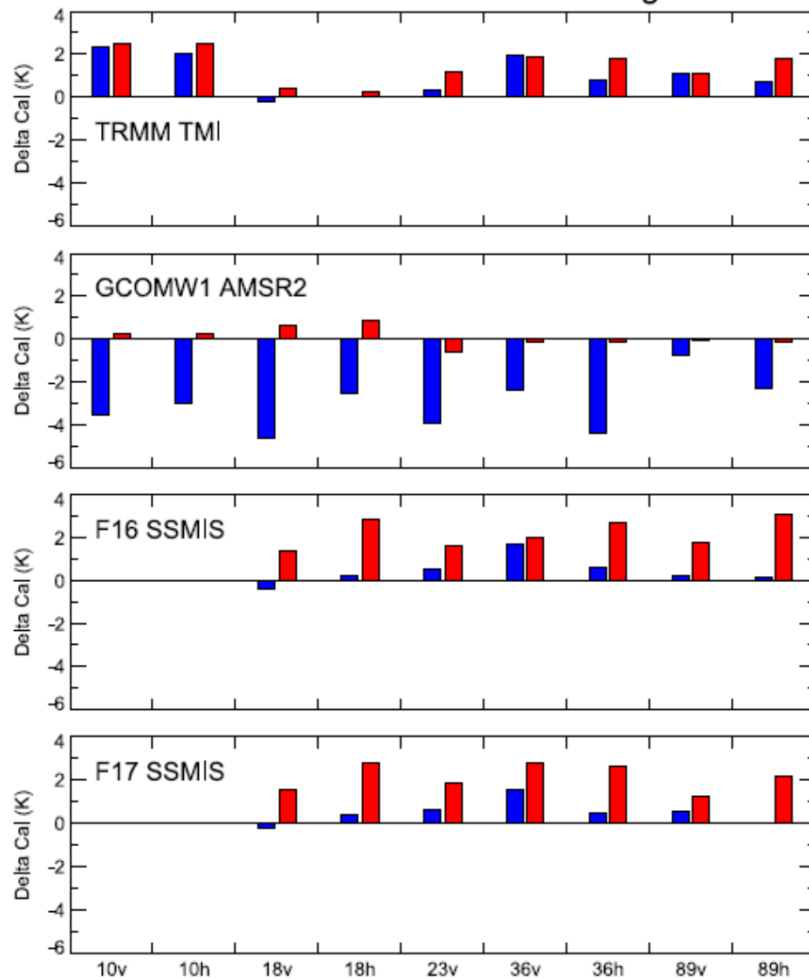
TABLE 9. On-orbit error analysis for GMI over ocean scenes. The results show an rms of all GMI channels. DSC stands for deep space calibration.

Error term	Static bias (K)	Time-varying error (1σ) (K)	Notes
Earth magnetic field correction	0	0.08	20% of rms for all channels
Instrument magnetic correction	0	0.02	20% of rms for all channels
Count bias correction	0.04	0	20% of DSC count bias, rms for all channels
Hot load	0.06	0.10	Preflight predict (1σ), scaled to 200-K ocean
Cold sky	0.04	<0.01	Preflight predict (rms), scaled to 200-K ocean
Nonlinearity	0.05	0	Preflight predict (1σ), scaled to 200-K ocean
Along-scan bias correction	0.00	0.02	20% of rms for all channels
Total T_A error	0.10	0.13	RSS of contributors
Inertial hold backlobe Earth T_B	0.07	<0.01	Results from 2-K error of $T_{B,eff}/2$
Inertial hold T_A calibration	0.21	0.02	Results from 0.2-K error of $(T_{Av} + T_{Ah})/2$
Inertial hold spillover annulus	0.07	<0.01	Results from 30% error on η_a
Total spillover correction error	0.23	0.02	RSS of contributors
X-pol correction error	0.03	0.03	25% of value, rms for all channels
Total T_B error (ocean scene)	0.25	0.14	RSS of T_A , spillover, and X-pol errors



X-Cal

GPM Imager Intercalibration Offsets vs. GMI





SNO/Double Difference

Satellite (sensor)	6–7 GHz	10 GHz	19 GHz	23 GHz	31–37 GHz	85–92 GHz	150–166 GHz	183 GHz
GPM (GMI)		10.65v	18.7v	23.8v	36.64v	89.0v	166.0v	183.31 ± 3v
Conical		10.65h	18.7h		36.64h	89.0h	166.0h	183.31 ± 7v
TRMM (TMI) ^a		10.65v	19.35v	21.3v	37.0v	85.5v		
Conical		10.65h	19.35h		37.0h	85.5h		
GCOM-WI (AMSR2)	6.925v	10.65v	18.7v	23.8v	36.5v	89.0v (A)		
	6.925h					89.0h (A)		
Conical	7.3v	10.65h	18.7h	23.8h	36.5h	89.0v (B)		
	7.3h					89.0h (B)		
DMSP F16–F19 (SSMIS)			19.35v	22.235v	37.0v	91.655v	150.0h	183.31 ± 1h
conical			19.35h		37.0h	91.655h		183.31 ± 3h
								183.31 ± 6.6h
MetOp-A/B, NOAA-18/NOAA-19 (MHS)						89qv	157.0qv	183.31 ± 1qh
cross track								183.31 ± 3qh
								190.31qv
Suomi-NPP (ATMS)				23.8qv	31.4qv	88.2 qv	165.5qh	183.31 ± 1.0qh
cross track								183.31 ± 1.8qh
								183.31 ± 3.0qh
								183.31 ± 4.5qh
								183.31 ± 7.0qh
Megha-Tropiques (SAPHIR)								183.31 ± 0.2qh
cross track								183.31 ± 1.1qh
								183.31 ± 2.8qh
								183.31 ± 4.2qh
								183.31 ± 6.8qh
								183.31 ± 11qh
Coriolis (WindSat) conical ^b		10.7v	18.7v		37.0v			
	6.8v	10.7h	18.7h	23.8v	37.0h			
	6.8h	10.7–3rd	18.7–3rd	23.8h	37.0–3rd			
		10.7–4th	18.7–4th		37.0–4th			

Incidence angle:

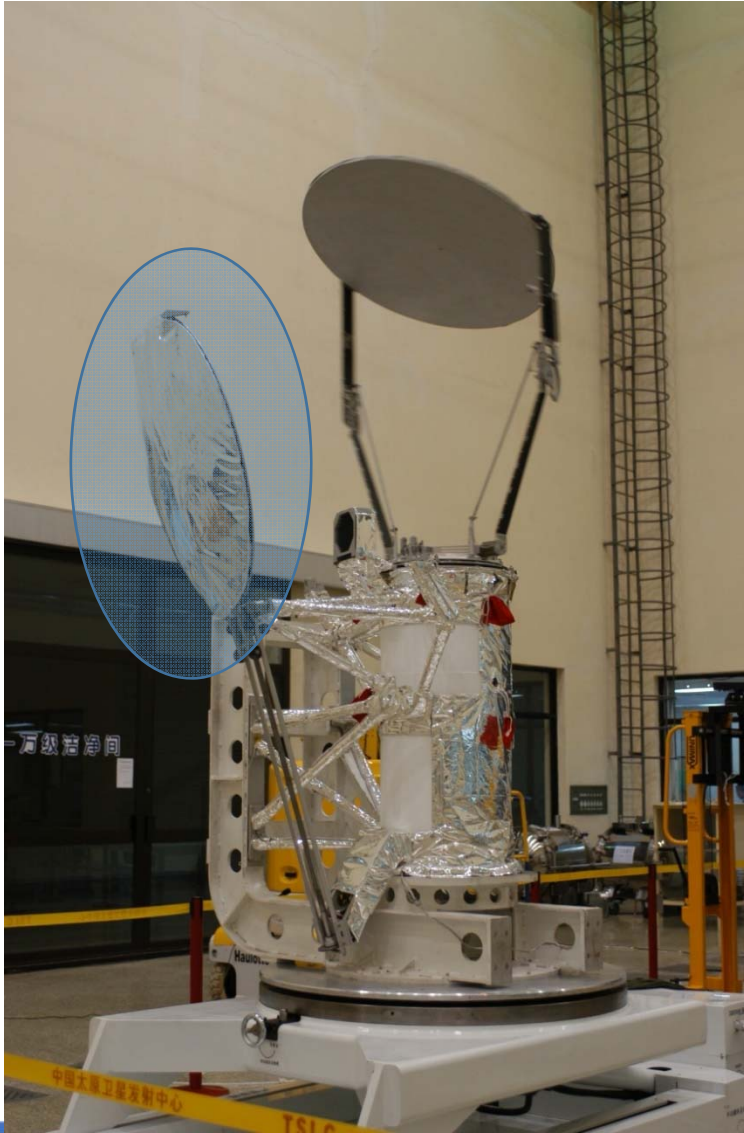
GMI: 52.821

MWRI: 53

AMSR2: 55



Error Source of MWRI Calibration



- **Back lobe of hot reflector**
- **Emission of hot reflector**
- **Hot load efficiency**
- **RFI Via cold reflector**
- **Non-linearity of receiver**





Roadmap of Recalibration

$$\begin{aligned} L_W &= \\ &= T_{EA}(1 - \eta_A) \\ &\quad - \eta_A \{ T_{ET}(1 - \eta_T) \\ &\quad + \eta_T [(1 - \varepsilon)T_{EC}(1 - \eta_H) + (1 - \varepsilon)T_H\eta_H \\ &\quad + \varepsilon T_R] \} \end{aligned}$$

$$L_{nl} = u \times G^2 \times (C_O - C_C) \times (C_O - C_W)$$

$$u = f(T_{rec}, AGC)$$

$$\begin{aligned} L_O \\ &= L_W + \frac{L_W - L_C}{C_W - C_C} \times (C_O - C_W) + L_{nl} + \Delta L_A \end{aligned}$$

- (1) Back-lobe
- (2) hot reflector ε ;
- (3) Hotload
- (4) non-linear correction

$$\Delta L_A = L_{sys} \left[\frac{1}{\Delta v \tau} + \left(\frac{\Delta G}{G} \right)^2 \right]^{1/2}$$





Calibration Equation and Parameters needs Corrected

$$L_O = L_W + \frac{L_W - L_C}{C_W - C_C} \times (C_O - C_W) + L_{nl} + \Delta L_A$$

Calibration Target

$$L_W = T_{EA}(1 - \eta_A) + \eta_A \{ T_{ET}(1 - \eta_T) + \eta_T [(1 - \varepsilon)T_{EC}(1 - \eta_H) + (1 - \varepsilon)T_H\eta_H + \varepsilon T_R] \}$$

Parameters
type



Reflector



Source

Receiver

$$L_{nl} = u \times G^2 \times (C_O - C_C) \times (C_O - C_W)$$

$$u = f(T_{rec}, AGC)$$

$$\Delta L_A = L_{sys} \left[\frac{1}{\Delta v \tau} + \left(\frac{\Delta G}{G} \right)^2 \right]^{1/2}$$



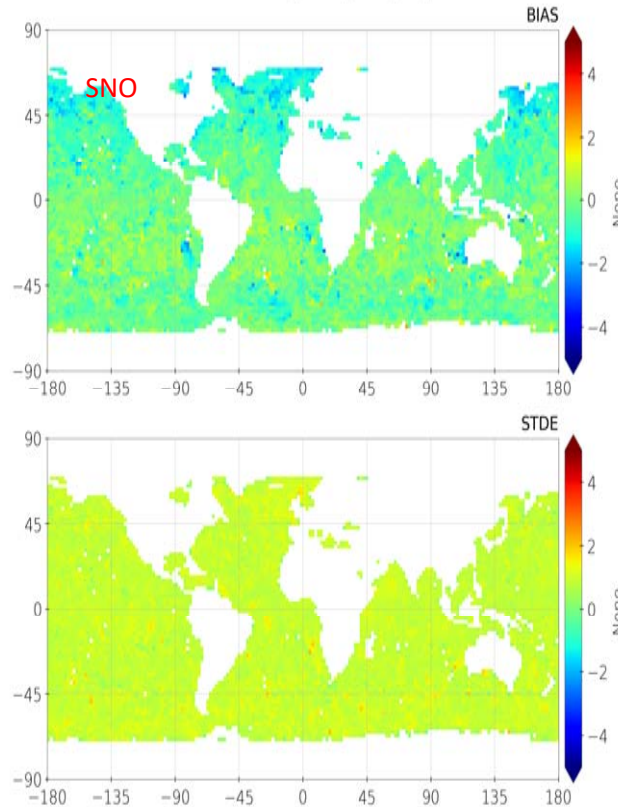
Receiver



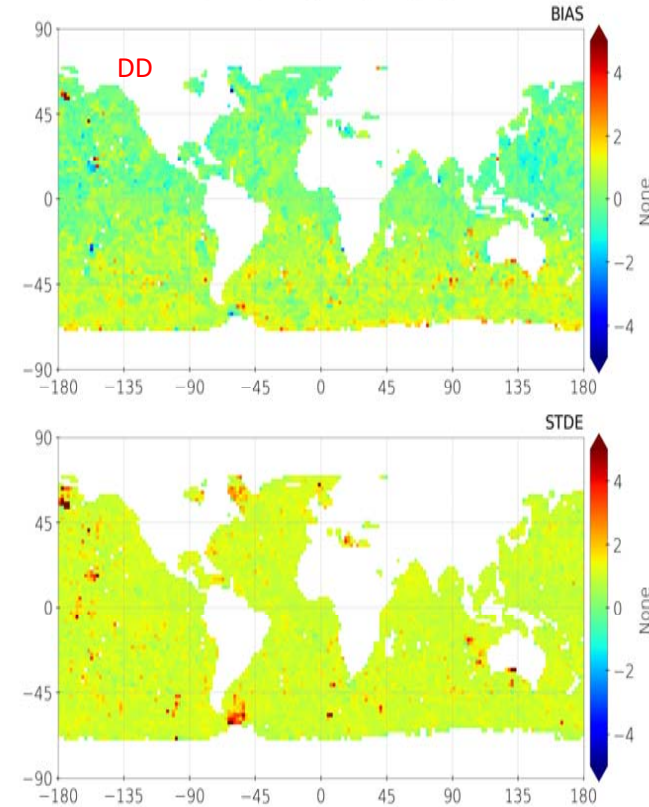


SNO and DD Between MWRI and GMI(89H)

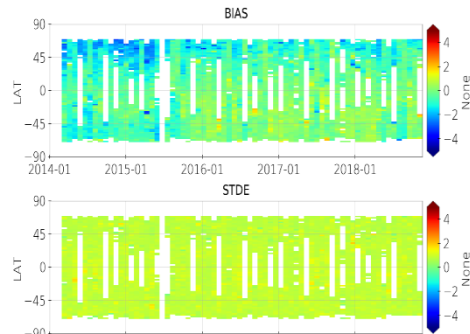
GEO-Statistics For (MWRI_Cal-GMI_Cal) 89.0_TH
data/mwri/FY3C_MWRI_GMI_V1_7x7.h5



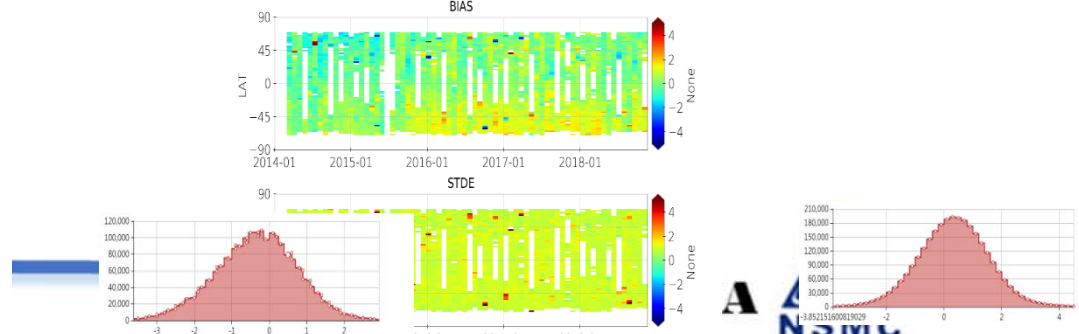
GEO-Statistics For (MWRI_Cal-MWRI_Simu)-(GMI_Cal-GMI_Simu) 89.0_TH
data/mwri/FY3C_MWRI_GMI_V1_7x7.h5

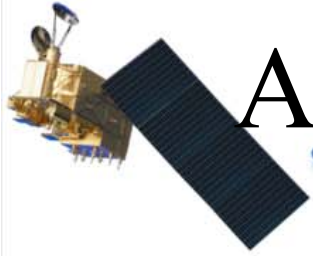


LAT-TIME-Statistics For (MWRI_Cal-GMI_Cal) 89.0_TH
data/mwri/FY3C_MWRI_GMI_V1_7x7.h5



LAT-TIME-Statistics For (MWRI_Cal-MWRI_Simu)-(GMI_Cal-GMI_Simu) 89.0_TH
data/mwri/FY3C_MWRI_GMI_V1_7x7.h5





Advantage of Double Difference

- MWRI $Bt^M B^M$
- GMI $Bt^G B^G$
- Real BT of SNO points: Bt^{TM}, Bt^{TG}
- SNO: $Bt^M - Bt^G = (Bt^{TM} + \sigma^M) - (Bt^{TG} + \sigma^G) = (Bt^{TM} - Bt^{TG}) + (\sigma^M - \sigma^G)$
- DD: $(Bt^M - B^M) - (Bt^G - B^G) = (Bt^{TM} + \sigma^M) - (Bt^{TG} + \sigma^G) - (B^M - B^G) = (Bt^{TM} - Bt^{TG}) + (\sigma^M - \sigma^G) - (B^M - B^G)$
 $(Bt^{TM} - B^M) - (Bt^{TG} - B^G) \cong (\sigma^M - \sigma^G)$

Difference of Model accuracy in
the 2 SNO points (~ 0)



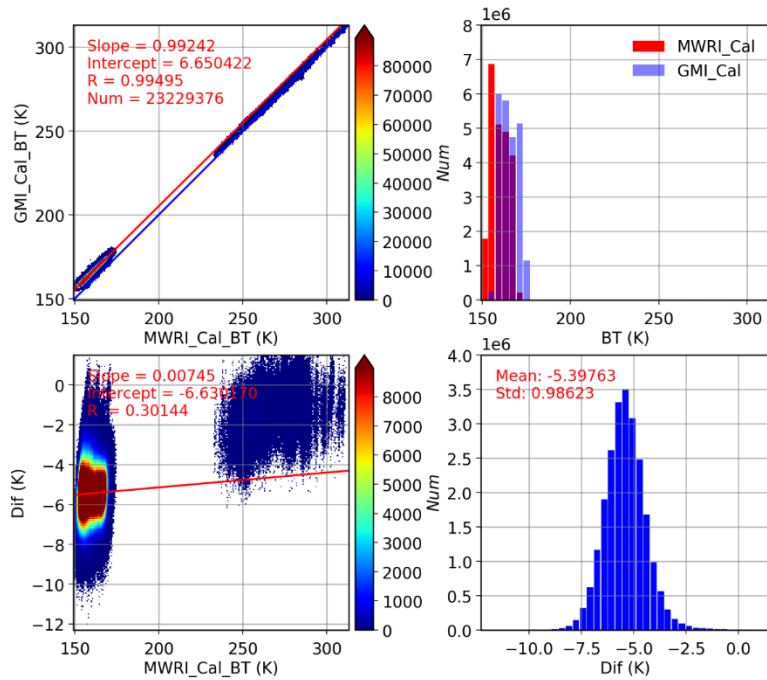


MWRI Recalibration Algorithm

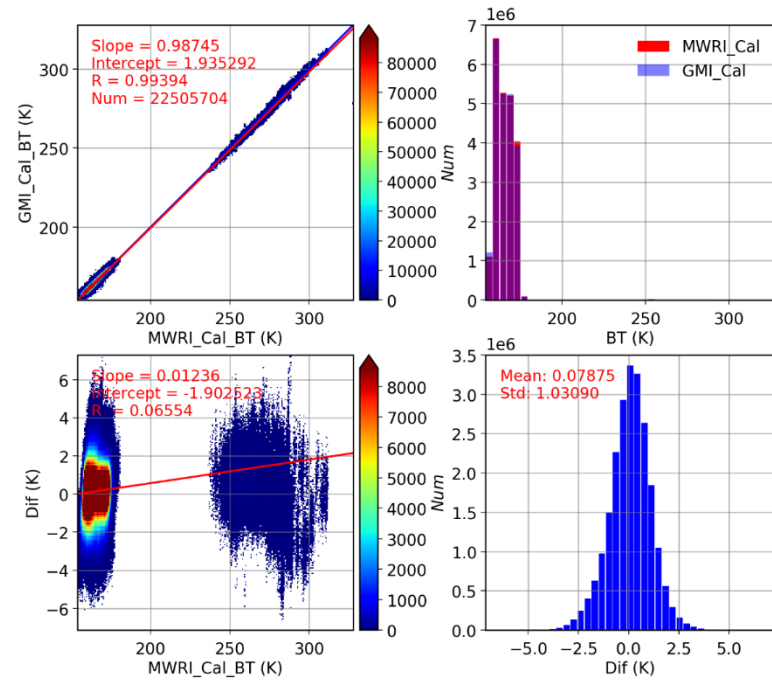
Algorithm	V1.0	V2.0	
		V1.1	V1.2
Back lobe	Using single orbit get back lobe factor	Global data	Improve data quality control
Hot reflector	Correction based on A/D Bias	Correction based on difference of physical temperature of hotload and hot reflector	Improve data quality control
Hot load	-	Using rain forest data to get better hot load parameter	Using data near the hotload temperature
Nonlinear	-	Using new back lobe, hot reflector and hot load parameters, and double difference data of ocean surface, do the correction of u, and the relation ship between u and receiver temperature.	Using different AGC
		Re-cal Parameters	Re-cal time series
FY-3B/MWRI		2014	2010-2019
FY-3C/MWRI		2014	2013-2020
FY-3B/MWRI		2018	2017-present



Correlation Analysis of Bright Temperature
FY3D_MWRI_GPM_GMI_V0-1.0 10.7_TV

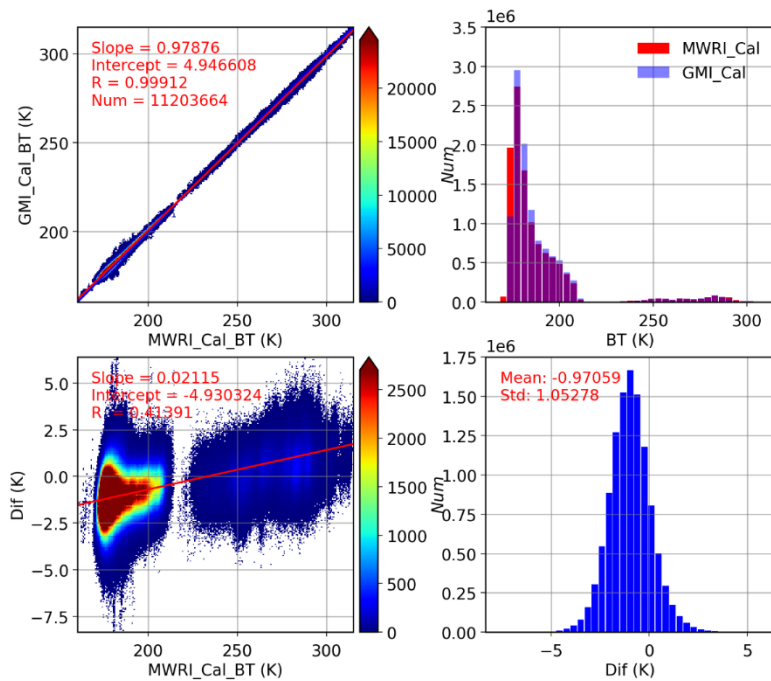


Correlation Analysis of Bright Temperature
FY3D_MWRI_GPM_GMI_V0-1.2 10.7_TV

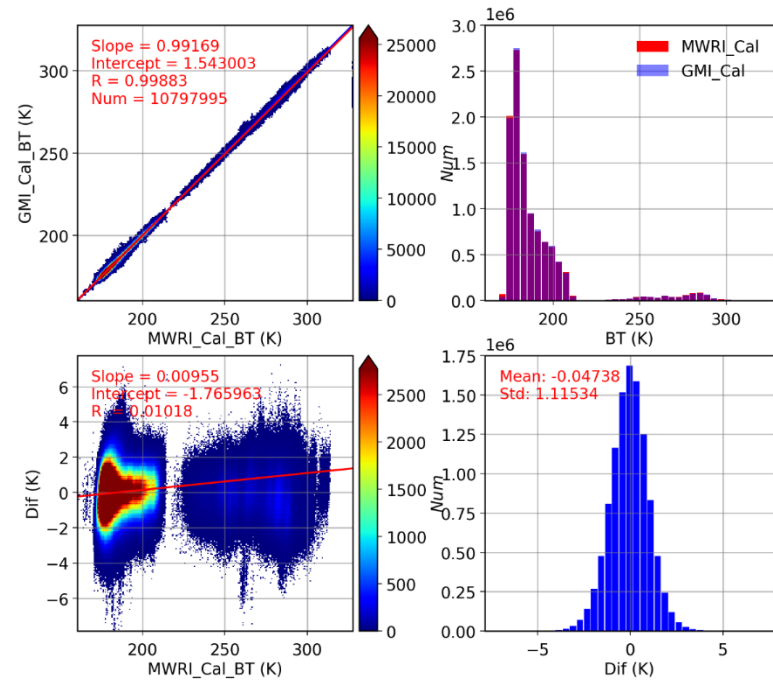




Correlation Analysis of Bright Temperature
FY3D_MWRI_GPM_GMI_V0-1.0 18.7_TV

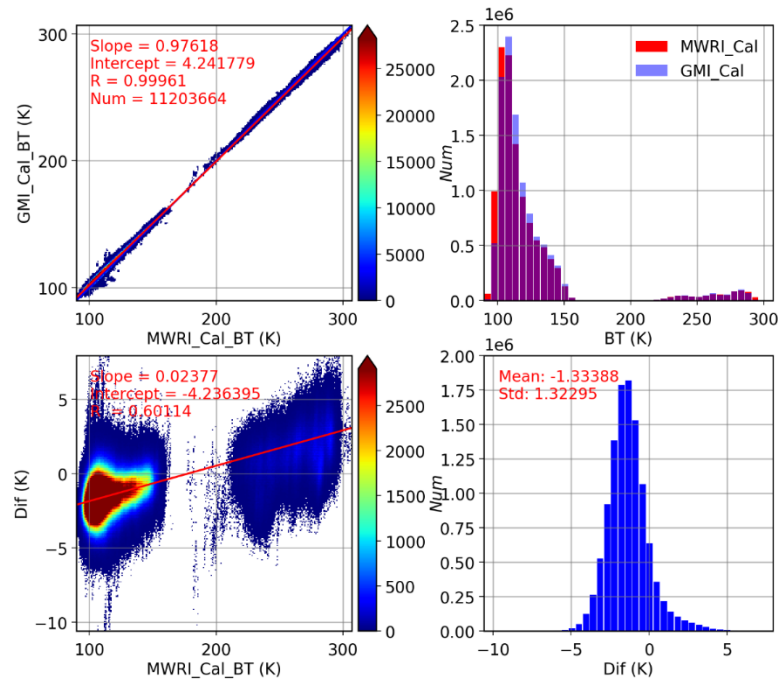


Correlation Analysis of Bright Temperature
FY3D_MWRI_GPM_GMI_V0-1.2 18.7_TV

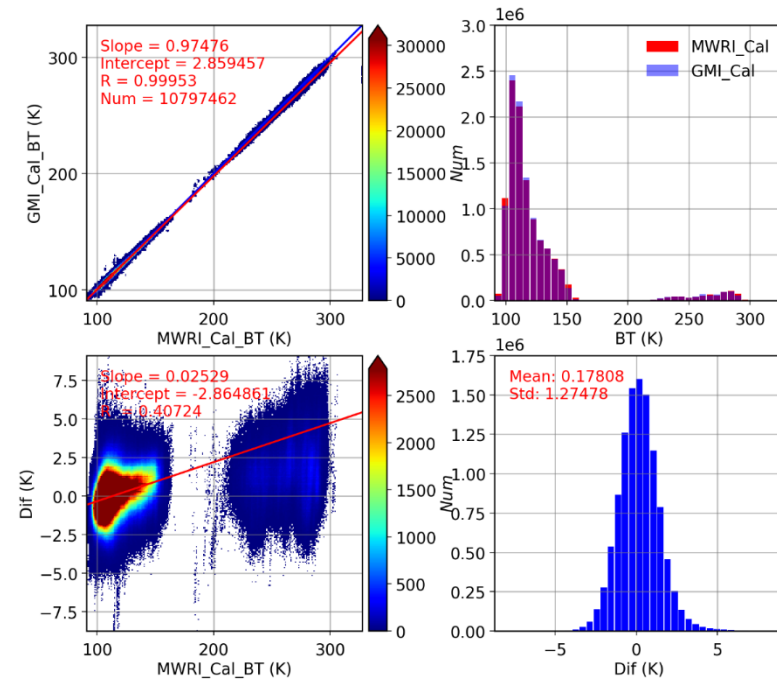




Correlation Analysis of Bright Temperature
FY3D_MWRI_GPM_GMI_V0-1.0 18.7_TH

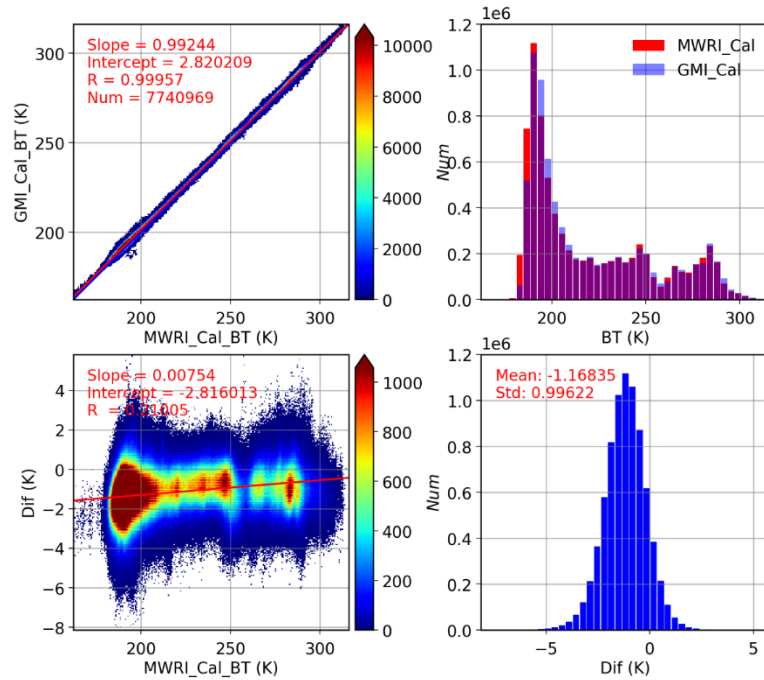


Correlation Analysis of Bright Temperature
FY3D_MWRI_GPM_GMI_V0-1.2 18.7_TH

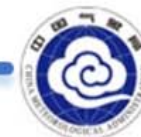
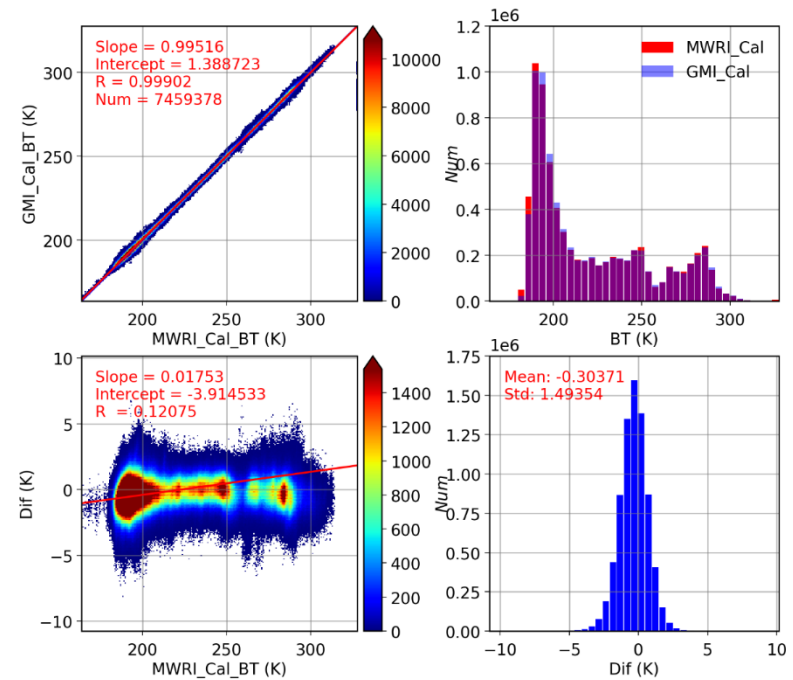




Correlation Analysis of Bright Temperature
FY3D_MWRI_GPM_GMI_V0-1.0 23.5_TV

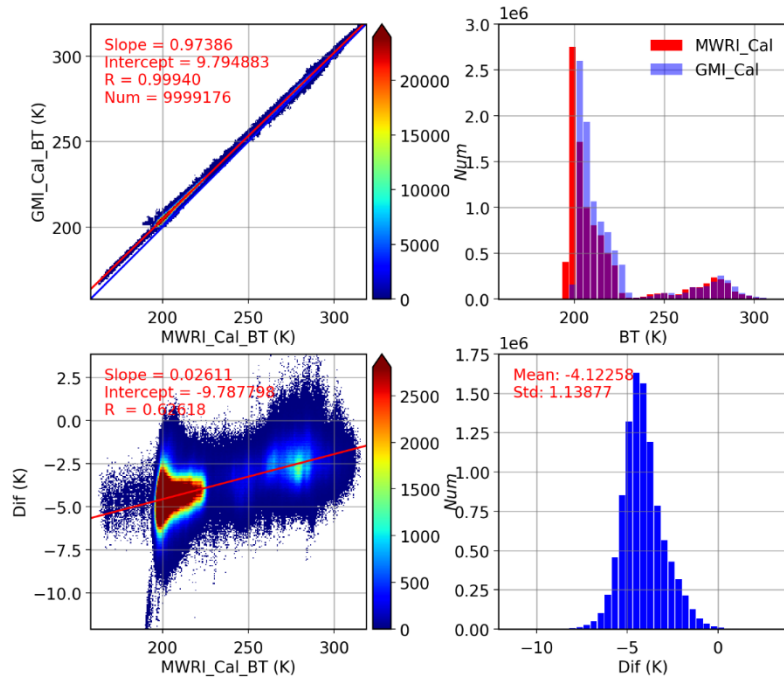


Correlation Analysis of Bright Temperature
FY3D_MWRI_GPM_GMI_V0-1.2 23.5_TV

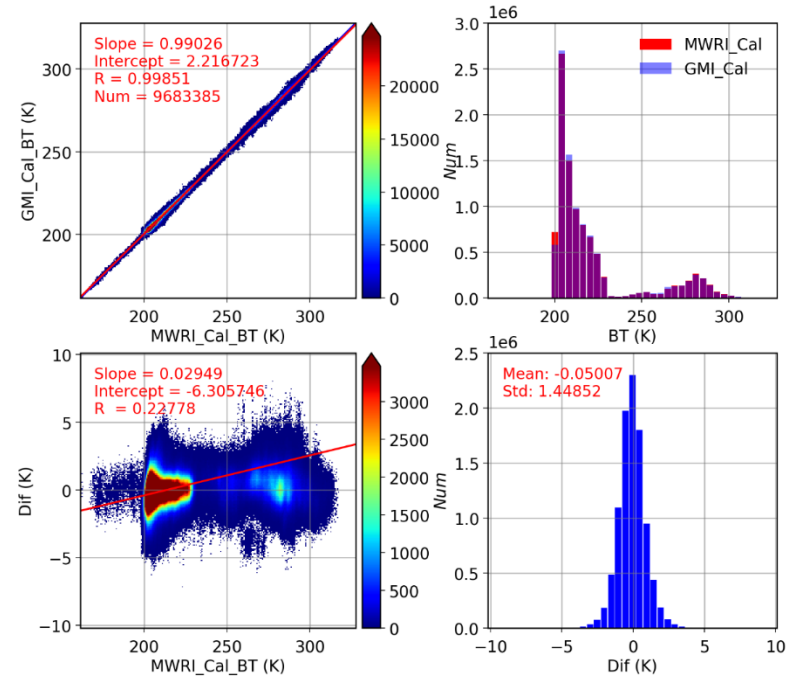




Correlation Analysis of Bright Temperature
FY3D_MWRI_GPM_GMI_V0-1.0 36.5_TV

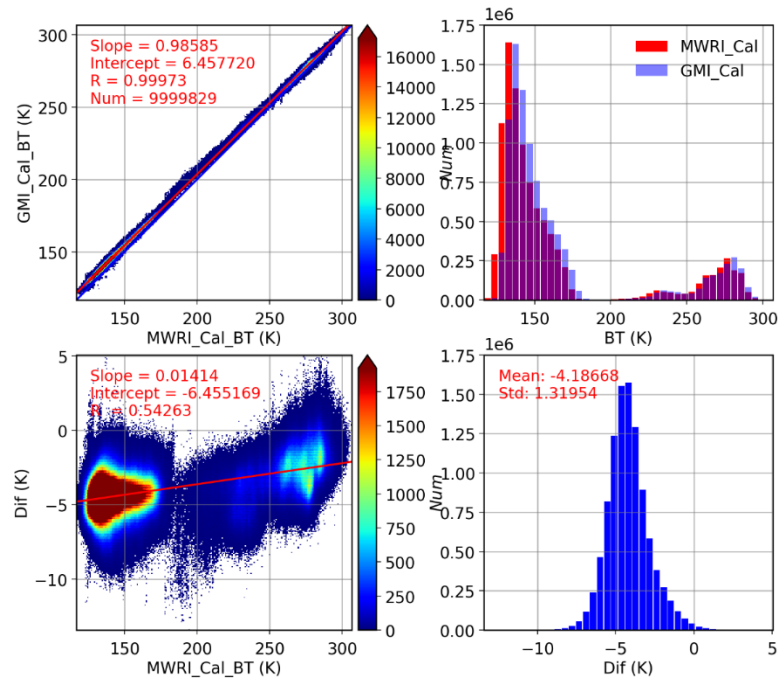


Correlation Analysis of Bright Temperature
FY3D_MWRI_GPM_GMI_V0-1.2 36.5_TV

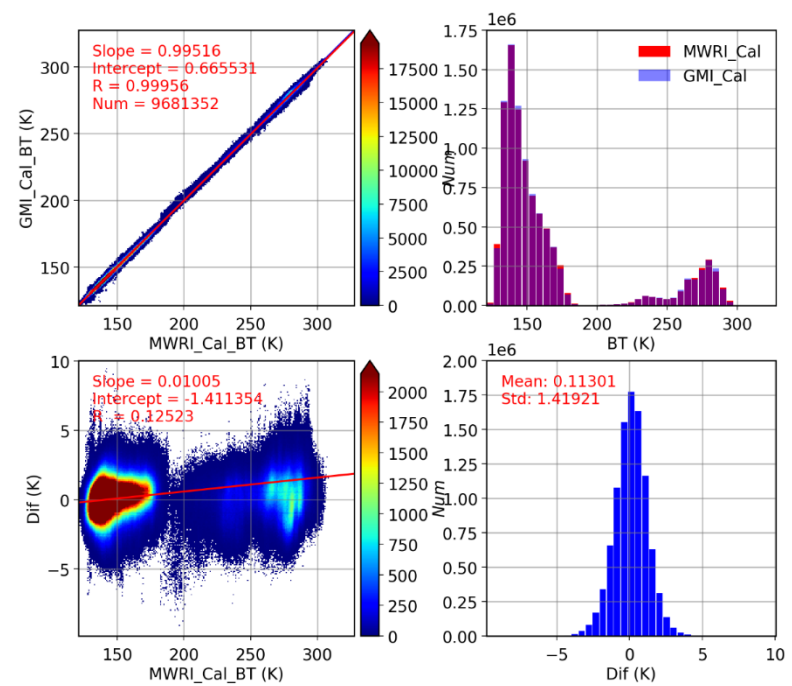




Correlation Analysis of Bright Temperature
FY3D_MWRI_GPM_GMI_V0-1.0 36.5_TH

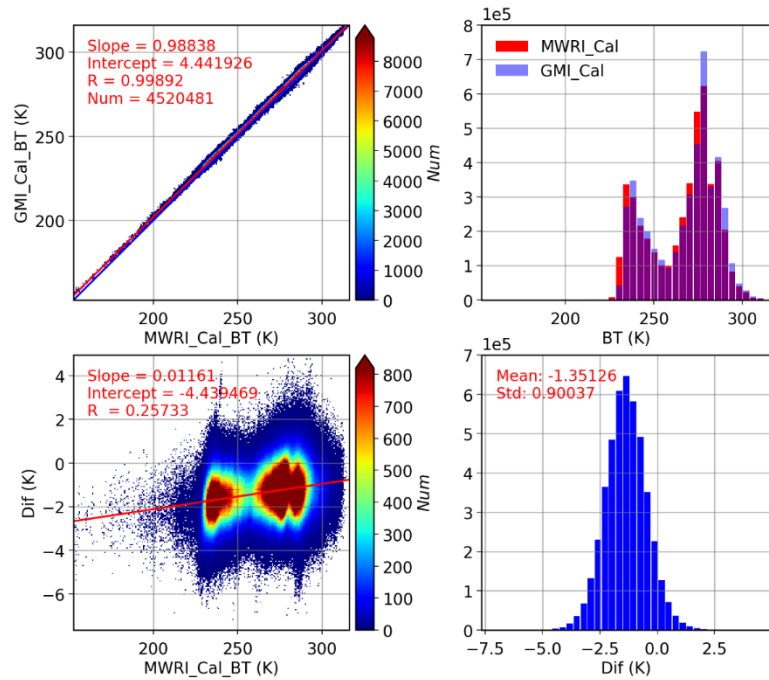


Correlation Analysis of Bright Temperature
FY3D_MWRI_GPM_GMI_V0-1.2 36.5_TH

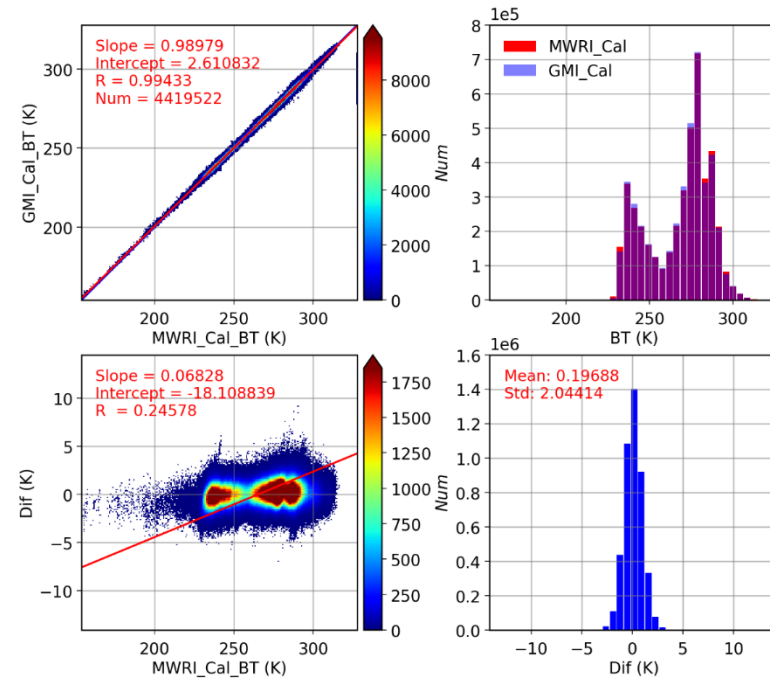




Correlation Analysis of Bright Temperature
FY3D_MWRI_GPM_GMI_V0-1.0 89.0_TV

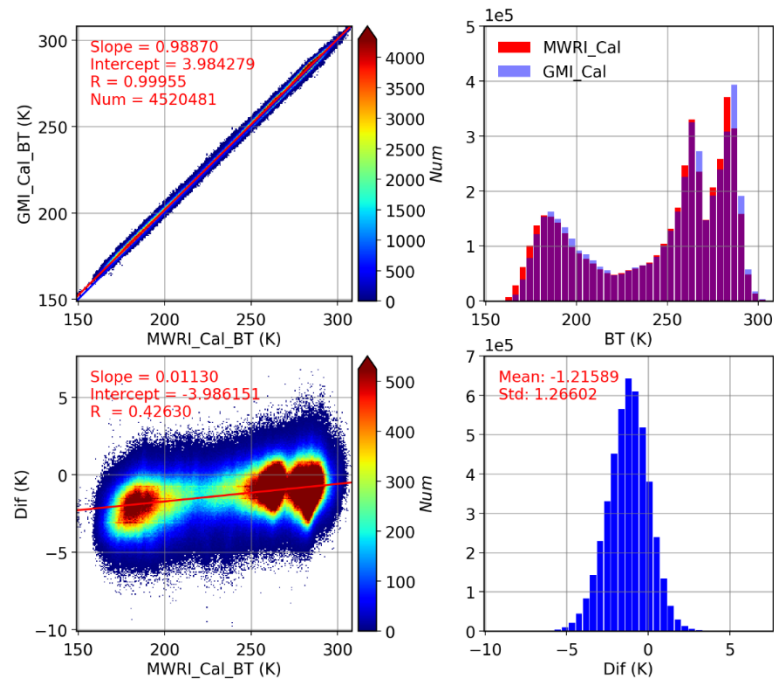


Correlation Analysis of Bright Temperature
FY3D_MWRI_GPM_GMI_V0-1.2 89.0_TV

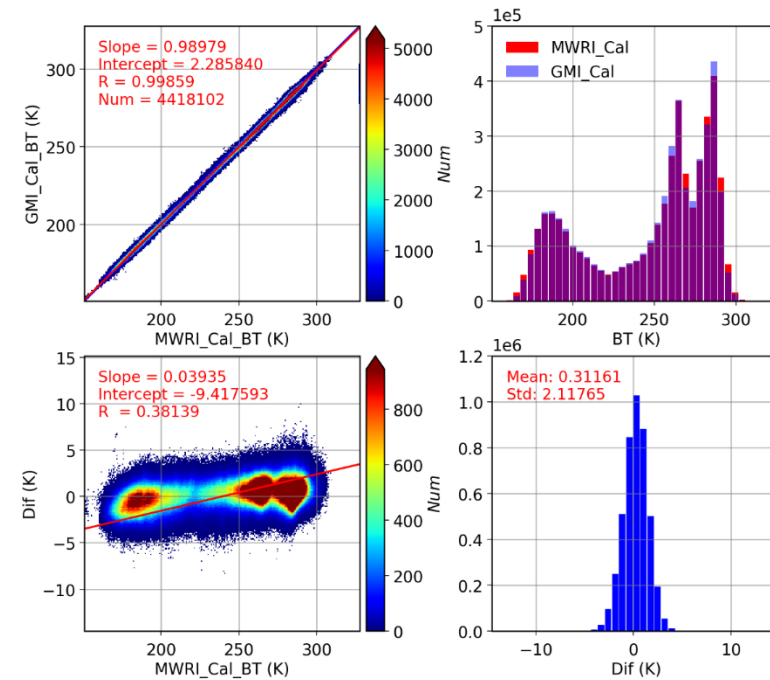




Correlation Analysis of Bright Temperature
FY3D_MWRI_GPM_GMI_V0-1.0 89.0_TH



Correlation Analysis of Bright Temperature
FY3D_MWRI_GPM_GMI_V0-1.2 89.0_TH





FY-3B/C/D MWRI time series

Operational

Recal V1.0

Recal V2.0

Diagram of Bright Temperature Dif (MWRI_Cal vs GMI_Cal)
MWRI_GPM_GMI_V0-0 10.7_TV

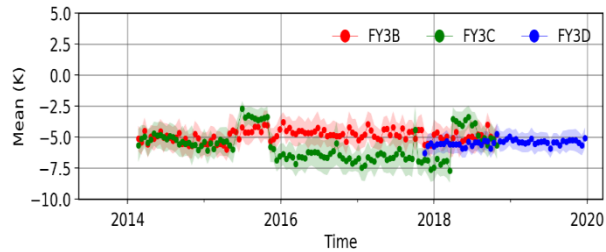


Diagram of Bright Temperature Dif (MWRI_Cal vs GMI_Cal)
MWRI_GPM_GMI 10.7_TV

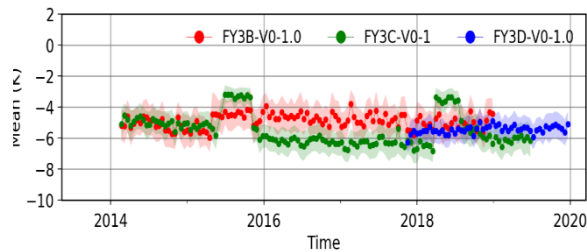


Diagram of Bright Temperature Dif (MWRI_Cal vs GMI_Cal)
MWRI_GPM_GMI_V0-1.2 10.7_TV

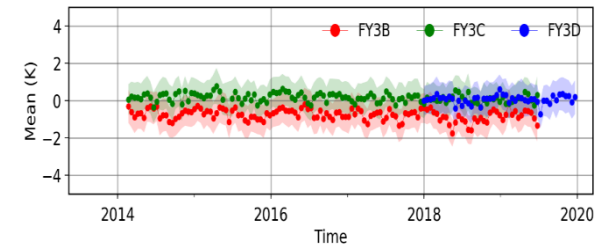


Diagram of Bright Temperature Dif (MWRI_Cal vs GMI_Cal)
MWRI_GPM_GMI_V0-0 18.7_TV

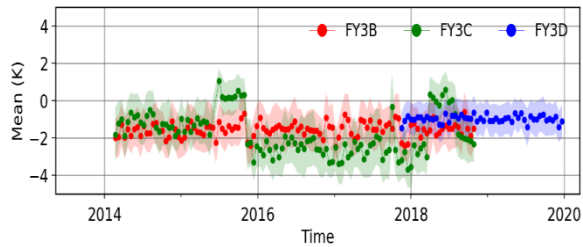


Diagram of Bright Temperature Dif (MWRI_Cal vs GMI_Cal)
MWRI_GPM_GMI 18.7_TV

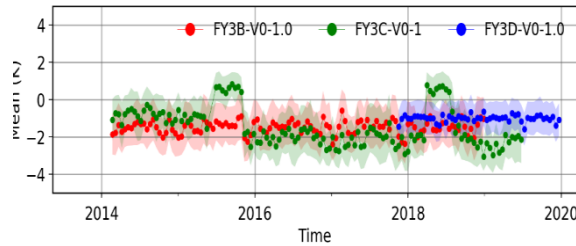


Diagram of Bright Temperature Dif (MWRI_Cal vs GMI_Cal)
MWRI_GPM_GMI_V0-1.2 18.7_TV

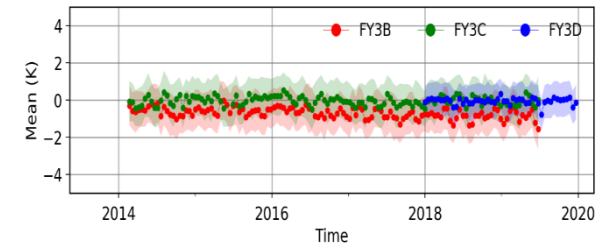


Diagram of Bright Temperature Dif (MWRI_Cal vs GMI_Cal)
MWRI_GPM_GMI_V0-0 23.5_TV

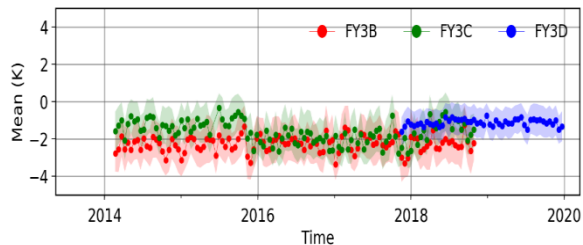


Diagram of Bright Temperature Dif (MWRI_Cal vs GMI_Cal)
MWRI_GPM_GMI 23.5_TV

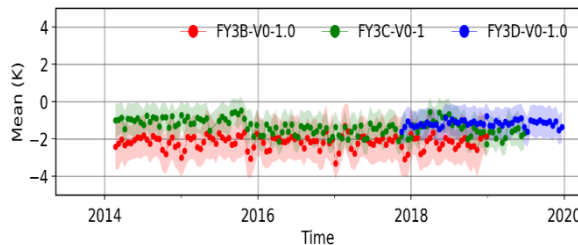
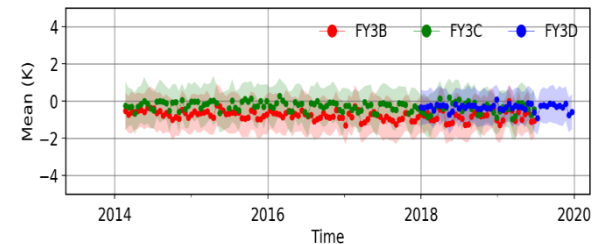


Diagram of Bright Temperature Dif (MWRI_Cal vs GMI_Cal)
MWRI_GPM_GMI_V0-1.2 23.5_TV





Operational

Diagram of Bright Temperature Dif (MWRI_Cal vs GMI_Cal)
MWRI_GPM_GMI_V0-0 36.5_TH

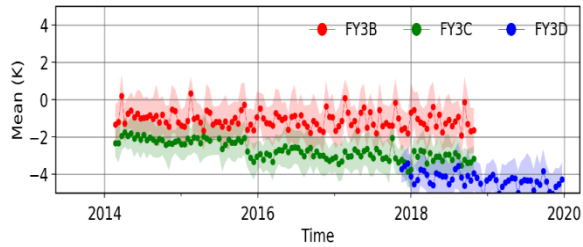


Diagram of Bright Temperature Dif (MWRI_Cal vs GMI_Cal)
MWRI_GPM_GMI_V0-0 89.0_TV

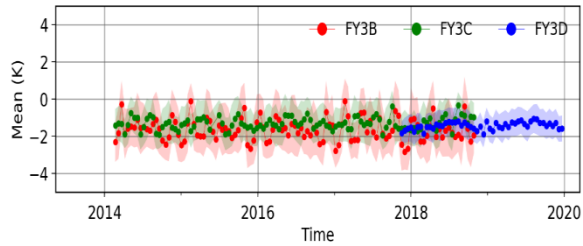
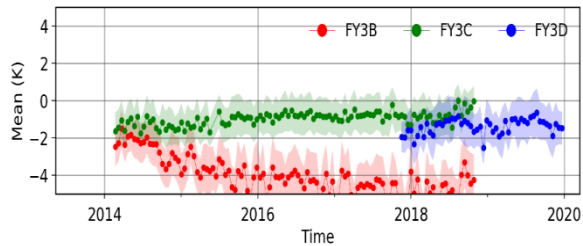


Diagram of Bright Temperature Dif (MWRI_Cal vs GMI_Cal)
MWRI_GPM_GMI_V0-0 89.0_TH



Recal V1.0

Diagram of Bright Temperature Dif (MWRI_Cal vs GMI_Cal)
MWRI_GPM_GMI 36.5_TH

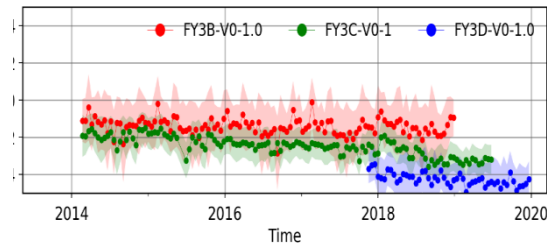


Diagram of Bright Temperature Dif (MWRI_Cal vs GMI_Cal)
MWRI_GPM_GMI 89.0_TV

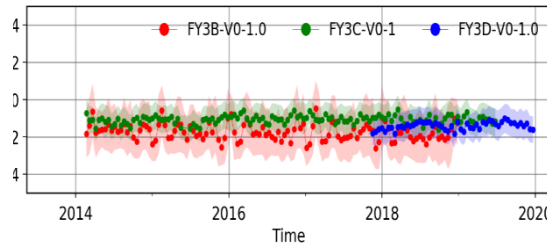
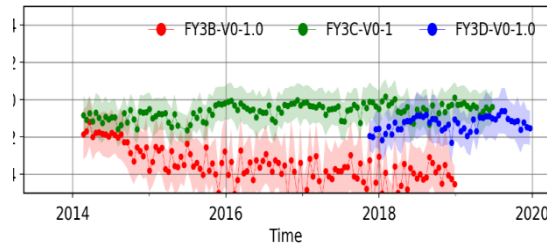


Diagram of Bright Temperature Dif (MWRI_Cal vs GMI_Cal)
MWRI_GPM_GMI 89.0_TH



Recal V2.0

Diagram of Bright Temperature Dif (MWRI_Cal vs GMI_Cal)
MWRI_GPM_GMI_V0-1.2 36.5_TH

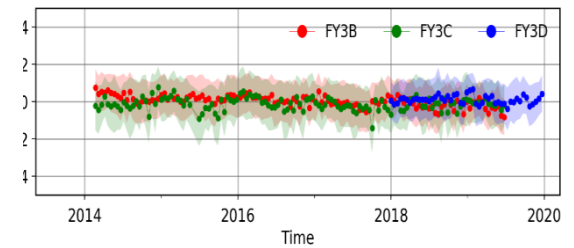


Diagram of Bright Temperature Dif (MWRI_Cal vs GMI_Cal)
MWRI_GPM_GMI_V0-1.2 89.0_TV

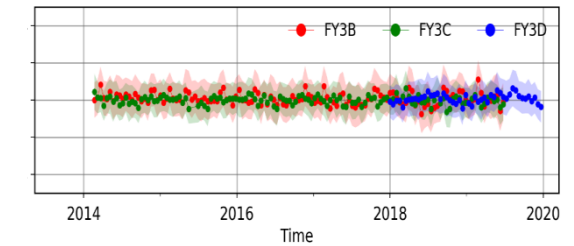
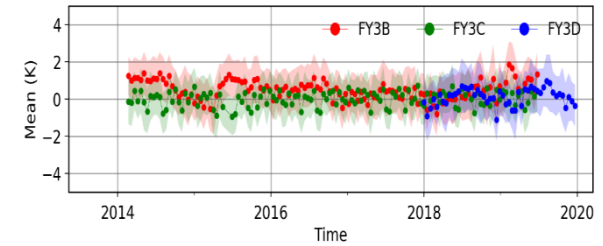
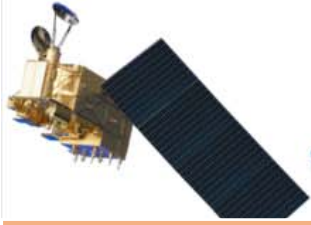


Diagram of Bright Temperature Dif (MWRI_Cal vs GMI_Cal)
MWRI_GPM_GMI_V0-1.2 89.0_TH





FY-3B/C/D MWRI

channel	Typical (K)	Mean of RMSE (K)		
		operational	Recal V1.0	Recal V2.0
FY-3B				
10V	166.2	5.00	5.00	1.15
10H	91.8	5.66	5.68	1.21
18V	119.4	1.91	1.87	1.26
18H	127.5	3.12	3.15	1.34
23V	224	2.51	2.46	1.29
36V	223.5	5.76	5.59	0.94
36H	172.1	1.62	2.03	1.10
89V	268.8	2.13	2.19	1.02
89H	248.8	4.24	3.85	1.34
FY-3C				
10V	166.2	5.85	5.85	0.88
10H	91.8	8.12	8.15	0.91
18V	119.4	2.27	2.72	1.07
18H	127.5	2.13	2.13	1.08
23V	224	1.95	1.95	1.10
36V	223.5	3.69	3.69	1.04
36H	172.1	2.87	2.87	1.26
89V	268.8	1.62	1.62	0.88
89H	248.8	1.38	1.38	1.15
FY-3D				
10V	166.2	5.51	5.51	0.91
10H	91.8	6.80	6.87	1.04
18V	119.4	1.32	1.33	0.93
18H	127.5	1.79	1.80	1.08
23V	224	1.41	1.45	1.02
36V	223.5	4.28	4.24	0.94
36H	172.1	4.41	4.39	1.09
89V	268.8	1.64	1.63	0.93
89H	248.8	1.82	1.76	1.33



Thanks

